SEISMIC DESIGN AND ASSESSMENT OF IRREGULAR 3-STOREY CONCENTRIC BRACED STEEL FRAME BUILDINGS

Nuno Gonçalo Cruz

DECivil, Instituto Superior Técnico, Universidade de Lisboa

April 2015

Abstract

The most common seismic-resistant steel frames built in areas of high seismicity are Moment Resisting Frames (MRFs), Concentric Braced steel Frames (CBFs) and Eccentrically Braced Frames (EBFs). This thesis aims at designing and evaluating the seismic response of X-Bracing CBFs steel structures in particular. The static design is accomplished according to European code EC3 (CEN 2005) while for seismic design an improved design procedure identified as Improved Force Based Design (IFBD) proposed by Villani et al. (2009) was carried out in complete accordance with the design criteria and detailing rules for frames with concentric braces prescribed by European code EC8 (CEN 2004). The IFBD procedure incorporates a proposal for an enhanced selection of the behaviour factor resulting in an improvement of the force-based procedure implemented in EC8 (through a linear dynamic analysis) and consequently aims at the achievement of more optimised and economical solutions.

A regular and an irregular in plan three storey CBF structures are studied and they are both laterally restrained, i.e. with concentrically braced frames all along its perimeter. These structures are designed according to IFBD procedure in accordance with EC8´s design criteria and detailing rules and in accordance with EC3's rules regarding the resistance of cross-sections and buckling resistance of members.

Afterwards the seismic assessment of both designed structures is defined through a non-linear static analysis, commonly referred to as Pushover Analysis. N2 method, adopted by EC8, is followed; it provides the inelastic deformation and structural strength demands imposed by the ground motion on both structures.

The same set of structures is also evaluated through a non-linear dynamic time history analysis. Although several attempts were made, its performance is only evaluated in terms of hysteretic response distribution along the height of both structures.

The non-linear modelling of CBF structures in this study, accomplished throughout the finite-element software OpenSees (PEER, 2006), was precursor at seismic evaluation in a tridimensional environment for structures of this nature.

Keywords: Concentric braced frames, *Improved Force Based Design*, non-linear static analysis, Seismic assessment, OpenSees

1. Introduction

Seismic behaviour of CBFs

Under a severe seismic action, MRFs solutions are very susceptible to large inter-storey drifts. This leads to structures of this nature being highly susceptible to instability due to second order effects and therefore require stockier steel members to respect the EC8 inter-storey drifts requirements. In comparison, CBFs are originally designed to meet both lateral stiffness and strength requirements with less steel tonnage than MRFs. Thus, CBFs are more cost effective solutions to resist lateral loads to low and medium rise steel buildings than MRFs. Though it is required controlling slenderness and overstrenght parameters of all braces across the CBF's structure to meet a ductile structural solution.

The lateral loads in CBFs are mainly conducted through axial loading in beams, columns and diagonal bracing members. Under cyclic loading, energy dissipation must be given only by the hysteretic response of braces ensuring that beams and columns have enough resistance to remain in the elastic range while the cyclic inelastic response occurs in braces. In short the main features of inelastic response in braces is to buckle in compression and yield in tension. According to Tremblay (2000) hysteretic response in braces varies with brace slenderness as follows: hysteresis energy dissipation in compression is lower on slender braces than in stockier braces, whereas, stocky braces are prone to exhibit local buckling of the cross section and brittle fracture at plastic hinge locations.

Capacity design and IFBD procedure applied to CBFs

Apart from providing additional resistance in beams and columns, implementing EC8 capacity design requirements (discussed in section 2.1) prevents the premature brace collapse under cyclic loading, prevents brittle failure of brace connections and enhances the energy dissipation on the bracing members. Therefore, capacity design ensures that CBFs can undergo several cycles in the

inelastic range without loss of structural integrity or excessive deformations, being then a ductile structural solution. EC8 specifies for CBFs the use of a model with tension-only diagonals (T/O brace model, as illustrated in **Fig. 1**.) for the evaluation of the design axial forces in the frames.

Current seismic codes make use of force-based design, which focuses in providing the structure with enough strength to resist the design earthquake. The ductility characteristics of the structure, which allows to reduce the strength level, is given by the behaviour factor *q*, an parameter defined by all seismic codes worldwide. In the EC8 the behaviour factor for CBFs is 4, regardless of the structure´s ductility class. The relation between top displacement and applied base shear illustrated in **Fig. 2** gives a deeper understanding of the behaviour factor, which can be written according to **equation 1**.

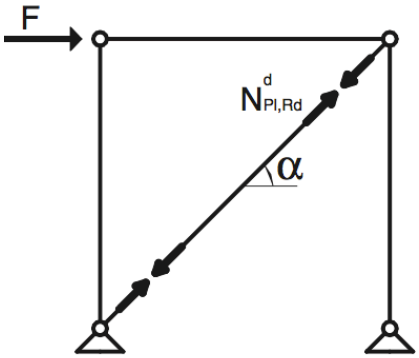

Fig. 1. Braced frame T/O model according to EC8 (Brandonisio et al. 2012)

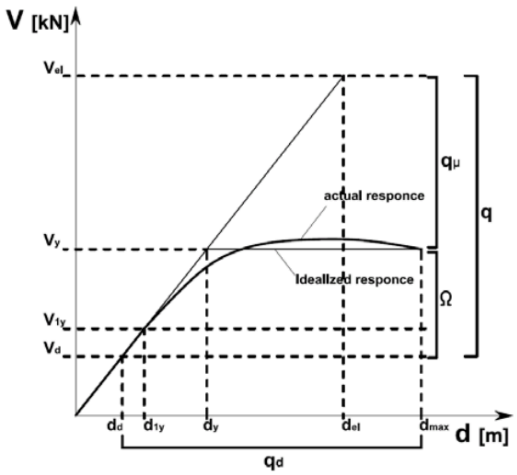

Fig. 2. Typical lateral response of a steel braced structure (Villani et al. 2009)

$$q = \frac{V_{el}}{V_d} = \frac{V_{el}}{V_y} * \frac{V_y}{V_d} = q_\mu * \Omega = \frac{V_{el}}{V_{1y}} \quad (1)$$

Where V_{el} is the elastic base shear, V_d is the design base shear and V_y the ultimate base shear. q_μ is the ductility component representative of the energy dissipation capacity of the structure (given by the bracing members in the CBFs) and Ω is the overstrenght component representative of the redistribution capacity (defined in EC8 by the ratio α_u/α_1), strain hardening of the material, the different between the expected and the design material strength, etc. Villani et al. (2009) proposal consists on a different order of the design steps (consideration of the serviceability deformation checks at the beginning of the design process) and the selection of the behaviour factor considering $V_d = V_{1y}$, i.e. the design base shear to be equal to the base shear that corresponds to the formation of the first plastic hinge in the frame. This estimation is made for each horizontal direction according

to **equation 2** and subsequently a decision on the global behaviour factor (regarding the tridimensional structure) is made.

$$q = \frac{V_{el}(Frame)}{V_{1y}} \quad (2)$$

Where $V_{el}(Frame)$ is the elastic base shear per direction obtained from the modal spectral analysis function of the period of vibration in that direction. V_{1y} is obtained when the axial load due to seismic action, $N_{Ed,E}$, plus the axial load due to gravity loads, $N_{Ed,G+0.3Q}$, equals the tension axial strength of the brace, $N_{pl,Rd}$, according to **equation 3**. V_{1y} is obtained from the smallest load factor λ_i of all braces of the frame.

$$N_{pl,Rd} = \lambda_i * N_{Ed,E} + N_{Ed,G+0.3Q} \quad (3)$$

2. Case Study

2.1 Description of the structures and seismic design

The improved design procedure is applied to the seismic design of both three-storey regular (**Fig. 3**) and irregular (**Fig. 4**) steel structures, known as REG and IRREG from now on, respectively. The identified frames located in the figures below are the bracing resisting frames.

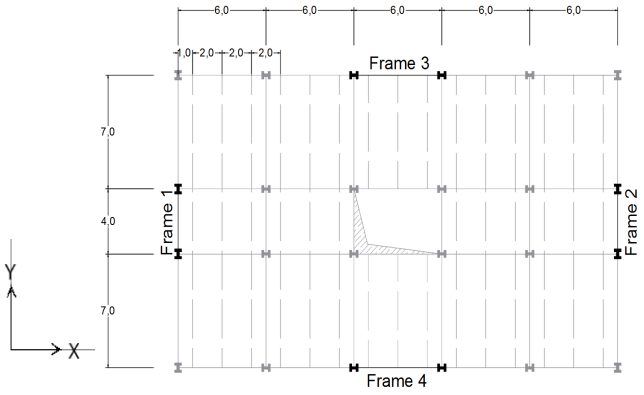

Fig. 3. Plan view of the three-storey regular structure, REG (dimensions in meters)

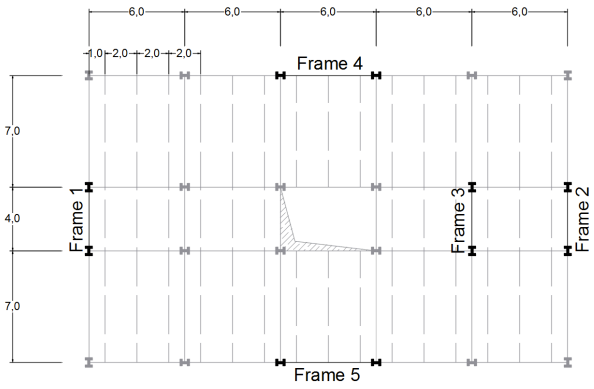

Fig. 4. Plan view of the three-storey irregular structure, IRREG (dimensions in meters)

In the Y direction the laterally resisting frames are illustrated in **Fig. 5** and in the X direction illustrated in **Fig. 6**. European sections of steel grade S355 for braces (CHS sections) and steel grade S275 for columns (HEB sections) and beams (IPE sections). Gravity loading design was initially carried out according to the provisions of EC3.

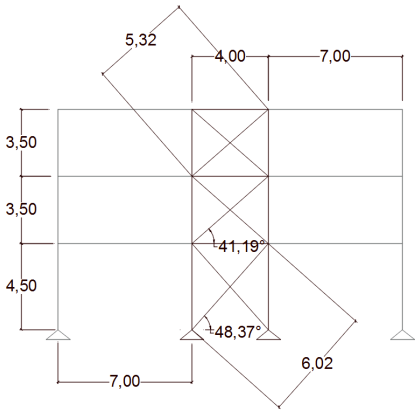

Fig. 5. Elevation view in Y direction of both structures

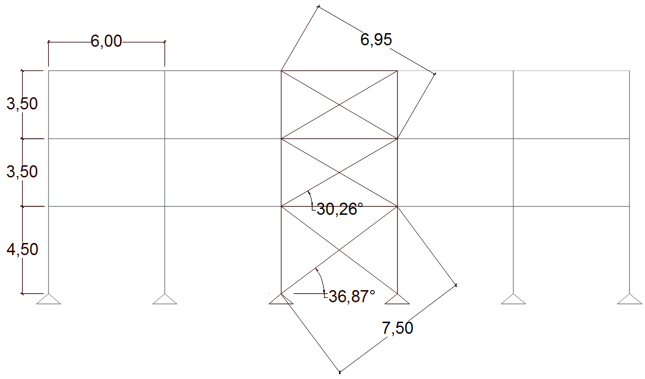

Fig. 6. Elevation view in X direction of both structures

The dead load considered is 3.93 kN/m^2, which include slab's self-weight and finishing, and a live load of 2.0kN/m^2 (floor 1 and 2) or 1.0kN/m^2 (floor 3). Seismic design was carried out for PGA=0.3g and a soil type of class B response spectrum according to EC8 classification to accomplish a linear dynamic analysis. Design action effects were calculated adding the gravity and the seismic effects divided by global behaviour factor assessed by the *IFBD* procedure. The gravity and seismic loads were evaluated and combined according to EN 1990 and EN1991 (CEN 2009) adding the values of the permanent action with the design value of seismic action and the quasi permanent value of variable action (a 0.3 value on all floors was used for the corresponding combination coefficient). In the seismic design the serviceability inter-storey drift ratio (IDR) was limited to 1.0% and the sensitivity coefficient (θ) was limited to 0.1. The capacity design of the dissipative members include the limitation of slenderness ratio for each brace, according to **equation 3**, and limited values of overstrenght among all braces along the height of each frame, according to the **equation 4**.

$$1.3 \leq \bar{\lambda} \leq 2.0 \tag{3}$$

$$\frac{\Omega_{max}}{\Omega_{min}} \leq 1.25 \tag{4}$$

Where the maximum overstrenght Ω_i (Ω_{max}), defined by **equation 5** (per brace in each floor of the frame), should not differ from the minimum value of $\Omega_i(\Omega_{\min}$) by more than 25%.

$$\Omega_i = \left(\frac{N_{pl,Rd,i}}{N_{Ed,i}}\right) \tag{5}$$

The capacity design of the non-dissipative members was conducted according to **equation 6** where Ω is the lowest value of **equation 5** in elevation of the frame and γ_{ov} is the overstrenght factor.

$$N_{pl,Rd} \geq N_{Ed,Gk+0.3Qk} + 1.1 * \gamma_{ov} * \Omega * N_{Ed,E} \tag{6}$$

The final member sizes for the REG and IRREG structures are displayed in **Table 1** and **Table 2**, respectively.

Table 1. Seismic design: Final member sizes for the REG structure

	Frames in Y direction (Frame 1 and 2)				Frames in X direction (Frame 3 and 4)			
Floor	**Ext. Col.**	**Int. Col.**	**Brace**	**Beam**	**Ext. Col.**	**Int. Col.**	**Brace**	**Beam**
3	HEB 200	HEB 300	CHS 139.7x3.2	IPE 300	HEB 200	HEB 300	CHS 139.7x3.2	IPE 330
2	HEB 200	HEB 300	CHS 139.7x6.3	IPE 330	HEB 200	HEB 300	CHS 139.7x4.0	IPE 360
1	HEB 200	HEB 300	CHS 139.7x8.0	IPE 330	HEB 200	HEB 300	CHS 139.7x5.0	IPE 360

Table 2. Seismic design: Final member sizes for the IRREG structure

	Frames in Y direction (Frame 1, 2 and 3)				Frames in X direction (Frame 4 and 5)			
Floor	**Ext. Col.**	**Int. Col.**	**Brace**	**Beam**	**Ext. Col.**	**Int. Col.**	**Brace**	**Beam**
3	HEB 200	HEB 300	CHS 114.3x3.2	IPE 300	HEB 200	HEB 300	CHS 139.7x3.2	IPE 330
2	HEB 200	HEB 300	CHS 139.7x6.3	IPE 330	HEB 200	HEB 300	CHS 139.7x4.0	IPE 360
1	HEB 200	HEB 300	CHS 139.7x8.0	IPE 330	HEB 200	HEB 300	CHS 168.3x5.0	IPE 360

The key parameters involved in the design of the REG and IRREG structures are listed in **Table 3** and **Table 4**, respectively. The most determinant frame per direction of each structure is displayed on the tables. The accidental torsional effects in the REG structure were taken into account by considering an accidental eccentricity.

Table 3: IFBD Design parameters for the REG structure

Frame ID	**Floor**	**T [s]**	**V_{el} [kN]**	**Drift Limit (0.01h)**	**V_d [kN]**	**q / $q_{adopt3D}$**	**θ**	$\bar{\lambda}$	**Ω_{min}**	**Ω_{max}**
Frame 1	3	0.84	1826.4	0.0239	692.6	2.36 / 3.5	0.0156	1.30	1.14	1.34
	2			0.0220			0.0255	1.47		
	1			0.0235			0.0273	1.69		
Frame 4	3	0.88	1883.8	0.0161	585.7	3.15 / 3.5	0.0174	1.88	1.05	1.61
	2			0.0222			0.0451	1.89		
	1			0.0281			0.0545	2.06		

Table 4: IFBD Design parameters for the IRREG structure

Frame ID	**Floor**	**T [s]**	**V_{el} [kN]**	**Drift Limit (0.01h)**	**V_d [kN]**	**q / $q_{adopt3D}$**	**θ**	$\bar{\lambda}$	**Ω_{min}**	**Ω_{max}**
Frame 1	3	0.72	1756.4	0.013	757.5	2.40 / 3.0	0.007	1.77	1.02	1.18
	2			0.018			0.013	1.47		
	1			0.024			0.017	1.69		
Frame 5	3	0.83	2020.0	0.017	703.6	3.0 / 3.0	0.015	1.88	1.05	1.32
	2			0.023			0.039	1.89		
	1			0.024			0.038	1.70		

From the two-dimensional estimation of the realistic behaviour factor for each direction, based on the updated dynamic characteristics and on the lateral capacity of the frame in each direction, the maximum value of both directions is the minimum value of *q* to be taken into account when it comes

to choose the behaviour factor for the tridimensional structure, i.e. global behaviour factor. The previous tables show that the global behaviour factor chosen for each structure is smaller than the global behaviour factor of 4 suggested by EC8, which indicates a limited level of inelastic demand to be imposed on both structures in comparison to the level proposed by EC8.

2.2 Numerical models

Both structures designed were modelled in OpenSees (PEER, 2006). Their columns, beams and braces are established as forced-based nonlinear beam-column elements (FBE) with 10 integration points, with spread plasticity and fiber cross-section formulation. The axial force-bending moment interaction curve is accounted for by integrating the uniaxial stress-strain relation for each cross-sectional fiber along the element length.

This formulation also allows plastic hinges to develop and considers Bauschinger effect. According to Uriz et al. (2008) a better mesh refinement (accomplished through a greater number of fibers) leads to a more accurate determination of inelastic deformation but its not significant for the global response. Beams and columns steel's nonlinearity is modelled through a bilinear stress-strain with 1.0% of strain hardening. For Braces is considered a Giuffre-Menegotto-Pinto model that accounts for accumulated plastic deformation, which means that the hysteresis loop follows the previous loading path for a new reloading curve, while deformations are cumulated. The braces are made of 10 FBE for the purpose of better refinement and to create an out-of-plane initial imperfection of L/1000, which leads to a larger out-of-plane deformation when the brace buckles in compression.

The behaviour of gusset plate connection at each brace end is accomplished by out-of-plane rotational spring and a torsional spring defined in the *zeroLength* element, connecting each end of the brace element with a rigid link known as *offset*. The rigid links simulate the remainder of gusset plate, its length being 0.1m and the properties of its elastic uniaxial material being 10 times higher than the contiguous nonlinear elements. Both springs are made of elastic uniaxial material with different Young's modulus ($E=1.0*10^{-3}$kPa for rotational spring; $E=1.0*10^{11}$kPa for torsional spring).

The described model is illustrated in Fig. 8, which shows the use of tension/compression diagonals (T+C model) in the structural scheme, unlike the scheme that was modelled in the design procedure (T/O model). **Fig. 7** illustrates the implemented model of the IRREG structure with depiction in blue of the global coordinate system adopted in OpenSees context. The construction of just the X-Bracing frame (and its contiguous beams and columns) on both REG and IRREG structures is intended to reduce computation time. The lack of the remainder of the structure it is not problematic because CBFs are not susceptible to second order effects.

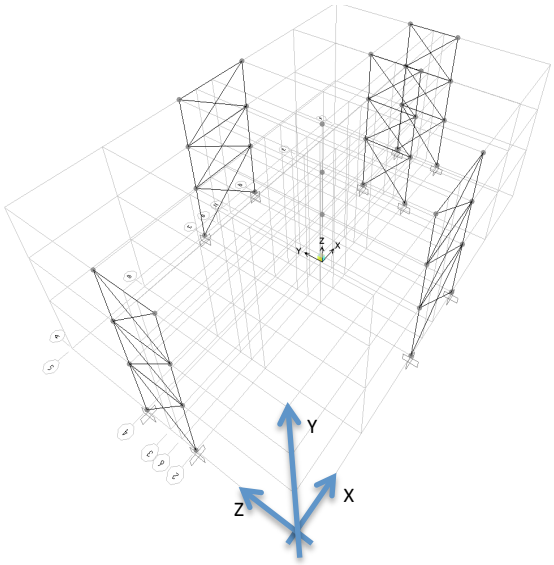

Fig. 7. OpenSees tridimensional model of the IRREG structure;

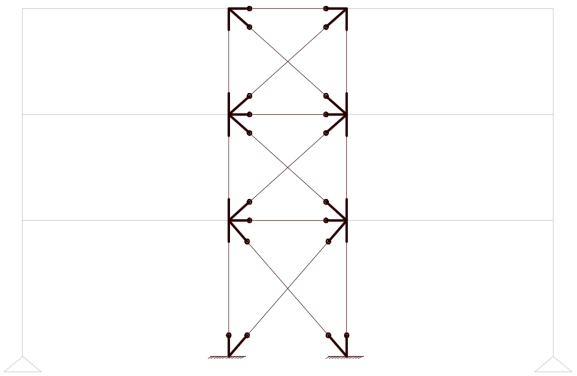

Fig. 8. OpenSees frame model

2.3 Nonlinear analysis procedures

Firstly a non-linear static (or pushover) analysis was conducted applying a modal and uniform pattern of lateral forces to the structure and controlling the displacement of a control node that usually is a roof node. This analysis enables the understanding of the structure's behaviour by showing its important properties highlighted in a capacity curve (base shear *vs.* top displacement), which provides information of the structure in terms of stiffness, overall strength and displacements.

According to (Krawinkler & Seneviratna 1998; Nogueiro et al. 2006) the main advantages of pushover analysis over the linear methods (linear static and linear dynamic analysis) are: i) consideration of non-linear behaviour which avoids the use of behaviour factor; ii) overall realistic force demands, particularly on potentially brittle elements such as brace connections and axial force demands on columns; iii) traces the sequence of yielding and failure on element level (which enables to identify critical regions subjected to high deformation demands that have to become focus of thorough detailing in seismic design) and structure level (force distribution due to inelastic behaviour that enables to identify strength discontinuities in plan and elevation); iv) accurate estimation of deformation demands for elements that have to deform inelastic in order to dissipate energy imparted to the structure by ground motions, such as the diagonals in CBFs.

Secondly a time-history analysis is performed by subjecting both structures to a set of fifteen records obtained from the PEER Ground-Motion Database. Each record is scaled in a manner that

the mean acceleration and displacement response spectra of all records approximately matches the EC8 Type 1 Ground type B response spectrum that governed the design. After several trials the convergence problem, which occurred under dynamic loading during the nonlinear stress-strain integration process, was not surpassed. This problem caused only one record successfully reaching its completion. Though the results obtained from the dynamic analysis in this work cannot be compared with the results attained from the pushover analysis; therefore, only the dynamic analysis' results regarding the hysteretic response at the braces are fully examined.

3. Discussion of Results

3.1 Nonlinear Static analysis

The lateral response of the set of frames in each direction is illustrated in terms of a capacity curve in **Fig. 9** for the REG structure and in **Fig. 10** for the IRREG structure. As shown in the figures below the modal load pattern produced lower shear forces for the same displacement values in comparison with the uniform load pattern, which means that the modal load pattern is chosen to be included in the N2 method.

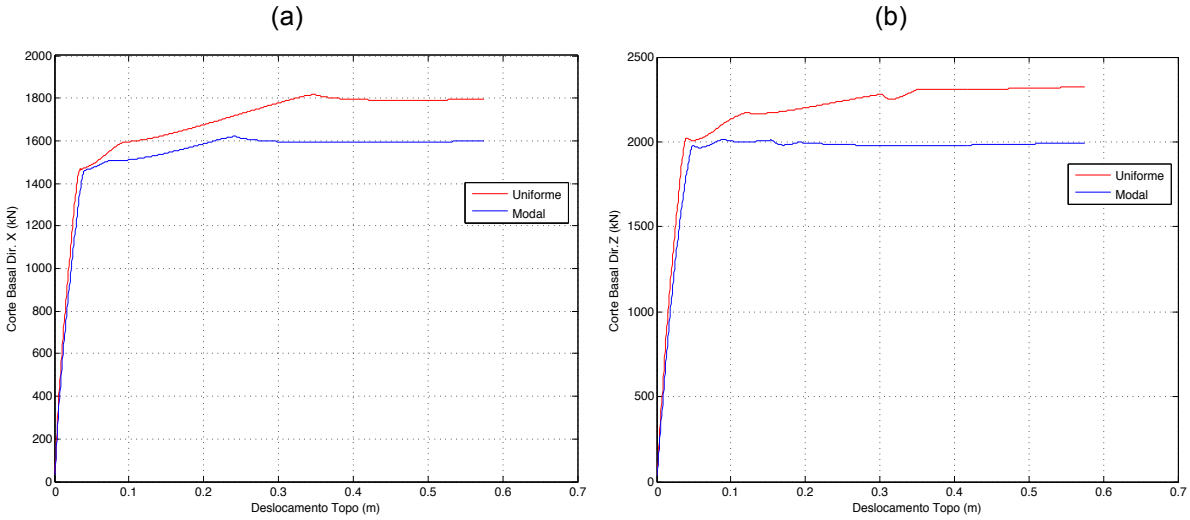

Fig. 9. REG structure's Pushover curves: (a) X direction and (b) Z direction

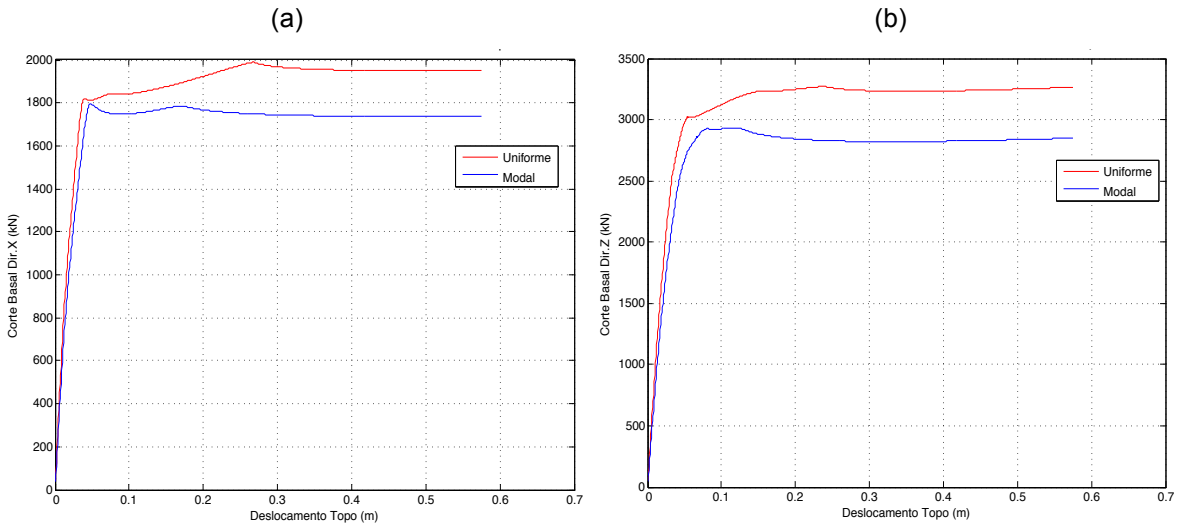

Fig. 10. IRREG structure's Pushover curves: (a) X direction and (b) Z direction

3.2 Linear dynamic analysis *vs.* Non-linear static analysis

Only for this section, a non-linear static analysis was performed on both structures considering the model of tension only diagonals (T/O) illustrated in **Fig. 1** in order to make a comparison between the design performed through IFBD procedure (Linear dynamic analysis) and non linear static analysis, regarding the assessment of the behaviour factor on both analyses.

Table 5 and **Table 6** show the comparison between analysis for REG and IRREG structures, respectively. The main parameters displayed on the tables have been described in section 1. The behaviour factor, *q*, is evaluated according to **equation 1** in the pushover analysis and compared with the behaviour factor, q_{2D}, estimated in the design.

REG Structure

As noticed, an excellent correlation is reached between the q_{2D}, estimated in the design for both directions, and the value of *q*, evaluated in the pushover analysis.

Table 5: REG structure, comparison between linear and non-linear analyses

		Linear dynamic analysis (T/O brace model)					**Non linear static analysis (T/O brace model)**					
		q_{2D}	**$q_{3DAdopt}$**	**T [s]**	**V_{EL} [kN]**	**V_D [kN]**	**T [s]**	**V_{1Y} [kN]**	**q**	**q_μ**	**Ω**	**V_Y [kN]**
REG	**Dir. X**	**3.15**	**3.5**	0.88	3767.7	1186.1	0.86	1204.5	**3.13**	2.65	1.18	1421.0
	Dir. Z	**2.36**		0.84	3652.8	1176.0	0.82	1569.2	**2.33**	2.17	1.07	1683.9

IRREG Structure

In this structure given that, for direction X, the global behaviour factor chosen in design matches the behaviour factor estimated in this direction ($q_{3D} = q_{2D}$) it is shown in **Table 6** that $V_D \approx V_{1Y}$.

Due to irregularity in plan the correlation (for both directions) between the value of $q_{2D,}$ estimated in design, is not similar to *q*, evaluated in the pushover analysis, although their values only differ 5% from each analysis, on both directions.

Table 6: IRREG structure, comparison between linear and non-linear analyses

		Linear dynamic analysis (T/O brace model)					Non linear static analysis (T/O brace model)					
		q_{2D}	$q_{3DAdopt}$	T [s]	V_{EL} [kN]	V_D [kN]	T [s]	V_{1Y} [kN]	q	q_μ	Ω	V_Y [kN]
IRREG	Dir. X	**3.0**	**3.0**	0.83	4040	1472.1	0.82	1424.2	**2.84**	2.62	1.08	1544.8
	Dir. Z	**2.4**		0.72	4261.6	1575.7	0.7	1937.8	**2.20**	1.74	1.26	2450.8

3.3 Seismic performance-based assessment

The seismic performance-based assessment consists in determining the target displacement, obtained from the intersection of the capacity curve of the structure with the seismic demand. For the corresponding target displacement, strength and deformation demands are compared with the available capacities at the performance levels of interest.

Nogueiro et al. (2006) prescribes as a performance-based assessment guideline, the maximum inter-storey drift ratio limit to be 2.5%. Therefore this ratio limit corresponds to a top displacement limit of 0.288m.

The target displacement was obtained following the N2 method proposed by Fajfar (2000) and adopted in EC8-Annex B. N2 method follows three main steps:

1) The pushover curves (considering the T+C brace model) illustrated in **Fig. 9** and **Fig. 10** were converted to an equivalent single degree of freedom (SDOF) system. A SDOF bi-linear capacity curve (elastic-perfectly plastic force-displacement relationship) was defined taking into account the following: i) the ultimate strength corresponds to an inter-storey drift of 2.5%; ii) initial stiffness of the idealized system was determined in such way that the areas under the pushover and the bi-linear curves are equal;
2) Seismic demand is defined based on the elastic response spectrum that induced the seismic design in form of an Acceleration-Displacement response spectrum (ADRS), valid for a SDOF system;
3) For the corresponding target displacement, bearing in mind the performance-based assessment guidelines, seismic assessment was carried out through the evaluation of the

following main performance parameters: horizontal displacements, inter-storey drifts and diagonals' axial response.

An iterative process was carried out until the final value of target displacement was obtained being the first iteration the top displacement equivalent to 2.5% of inter-storey ratio.

REG Structure

For REG structure **Fig. 11a** and **12a** show graphically the determination of the target displacement for modal load pattern in a SDOF system in X direction and Z direction, respectively. To determine the target displacement corresponding to MDOF system, shown by **Fig. 11b** and **12b** in X direction and Z direction, respectively, the target displacement of the equivalent SDOF system has to be multiplied by the Γ factor (2.88 and 2.86 for X direction and Z direction, respectively) In these figures is illustrated the base shear corresponding to the formation of the first plastic hinge (V_{1Y}). Both bilinear capacity curve and MDOF pushover curve are displayed until the target displacement.

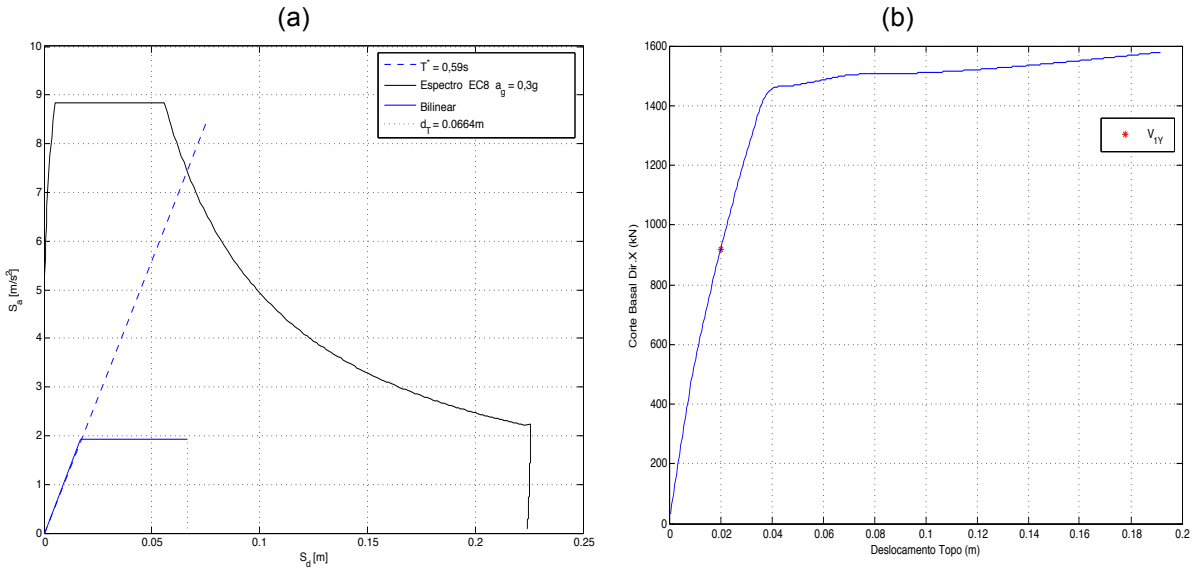

Fig. 11: REG structure X direction, (a) Target displacement in SDOF system and (b) Capacity Curve until target displacement in MDOF system.

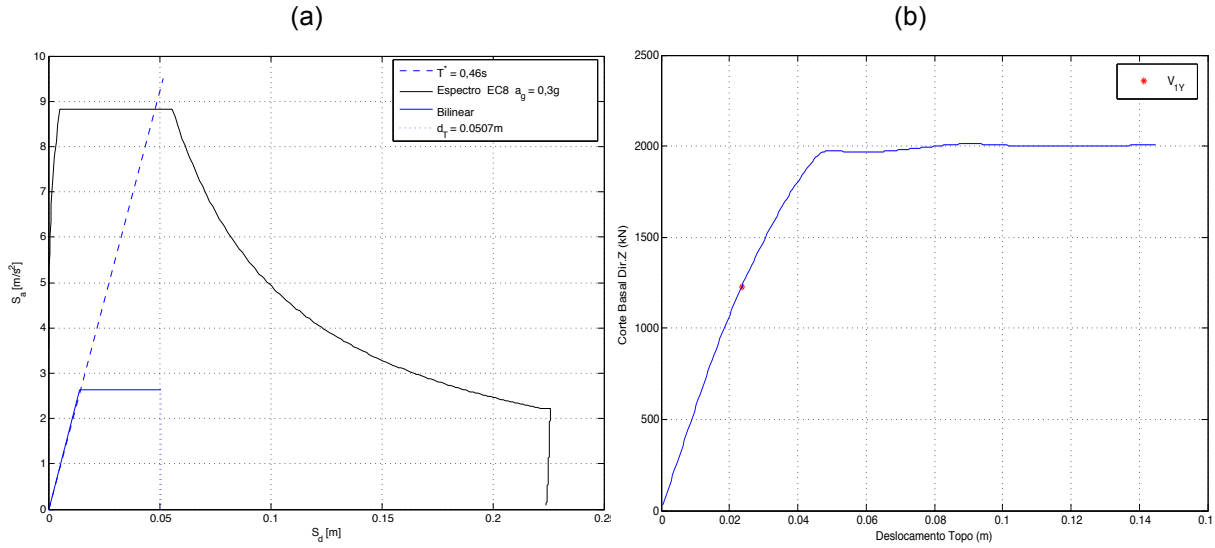

Fig. 12: REG structure Z direction, (a) Target displacement in SDOF system and (b) Capacity Curve until target displacement in MDOF system.

Table 7 compares the target top displacement for the N2 method performed on both directions with the reference value displayed in the last column. Given that the N2 method is an iterative process, the reference value is considered as the first iteration of such process implemented on both directions. **Fig. 13** and **14** show the results of seismic assessment in terms of (a) horizontal displacements and (b) inter-storey drifts along height for X direction and Z direction, respectively. These figures reveal that the maximum inter-storey drifts occur in the first storey.

Although the following table implies the seismic demand is below the structures capacity in both directions, **Fig. 13a** shows that the inter-storey drift of the first storey surpasses the reference value of 2.5% in X direction which indicates that the braces' connections should be redesigned in this direction.

Table 7. REG structure, Horizontal top displacements

		δ_{target} (m)	Limit δ_{top} (m) [0.025*H]
REG	Dir. X	0.191	0.288
	Dir. Z	0.145	

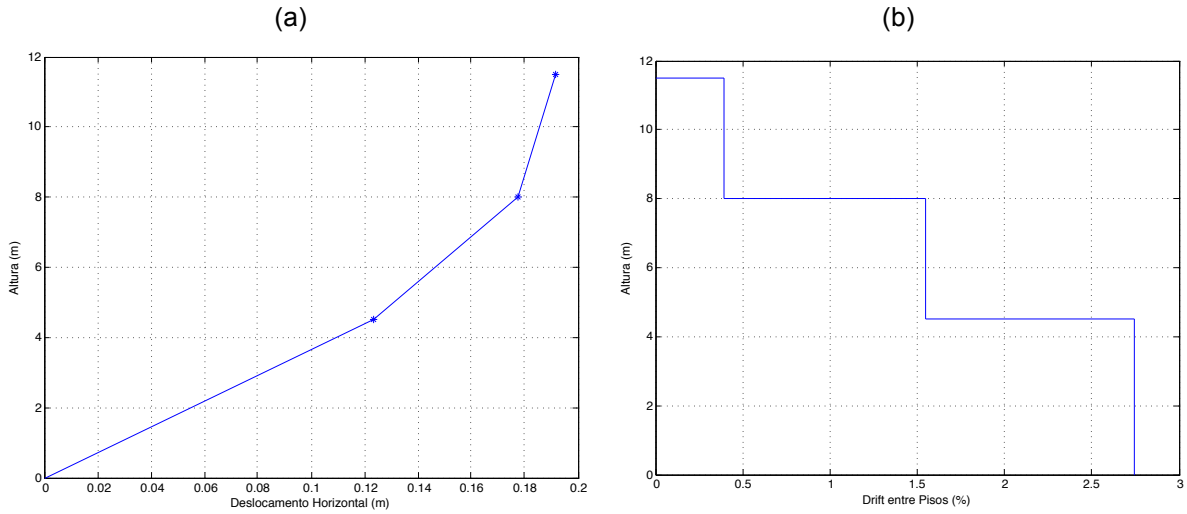

Fig. 13: REG structure X direction graphs for Target displacement, (a) Maximum horizontal displacements and (b) Inter storey drifts.

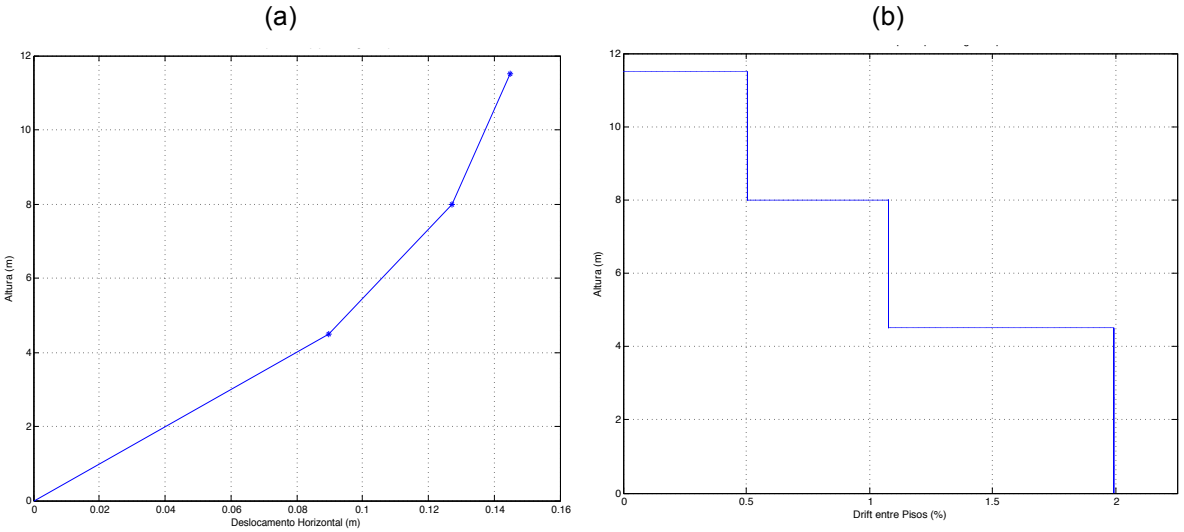

Fig. 14: REG structure Z direction graphs for Target displacement, (a) Maximum horizontal displacements and (b) Inter storey drifts.

Fig. 15a and **15b** illustrates the diagonals' axial force *vs.* top displacement (braces in tension and compression) for each storey and it is also illustrated the corresponding target displacement for X direction and Z direction, respectively. It is worth noticing that all diagonals, other than the diagonal in tension located in storey 3, are performing in the inelastic range, which indicates ductile frames on both directions of the REG structure.

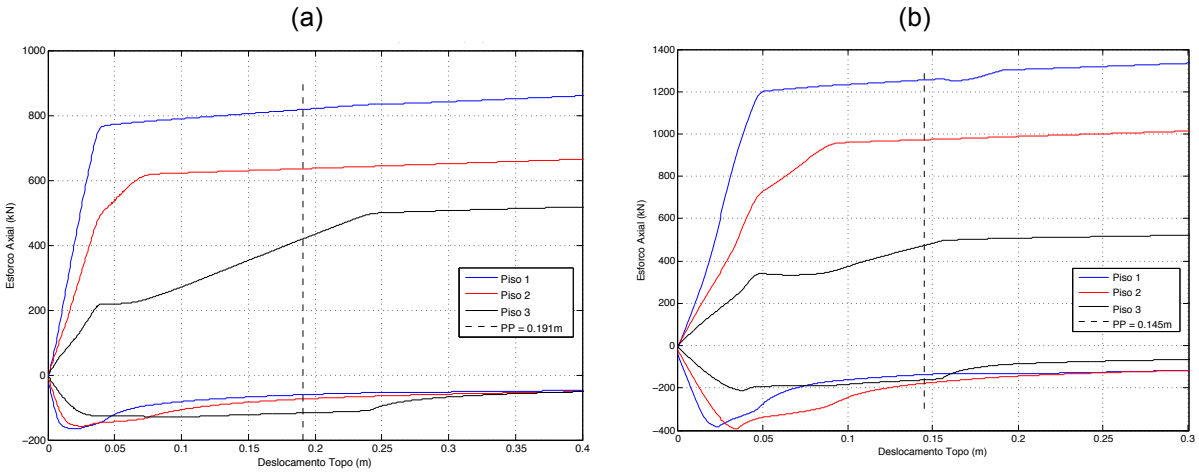

Fig. 15: REG structure, Diagonals response (axial force *vs.* top displacement) and representation of the corresponding target displacement in (a) X direction and (b) Z direction

IRREG Structure

For IRREG structure **Fig. 16a** and **17a** show graphically the determination of the target displacement for modal loading in a SDOF system in X direction and Z direction, respectively. To determine the target displacement corresponding to MDOF system, shown by **Fig. 16b** and **17b** in X direction and Z direction, respectively, the target displacement of the equivalent SDOF system has to be multiplied by the Γ factor (2.88 and 2.86 for X direction and Z direction, respectively). In these figures is illustrated the base shear corresponding to the formation of the first plastic hinge (V_{1Y}). Both bilinear capacity curve and MDOF pushover curve are displayed until the target displacement.

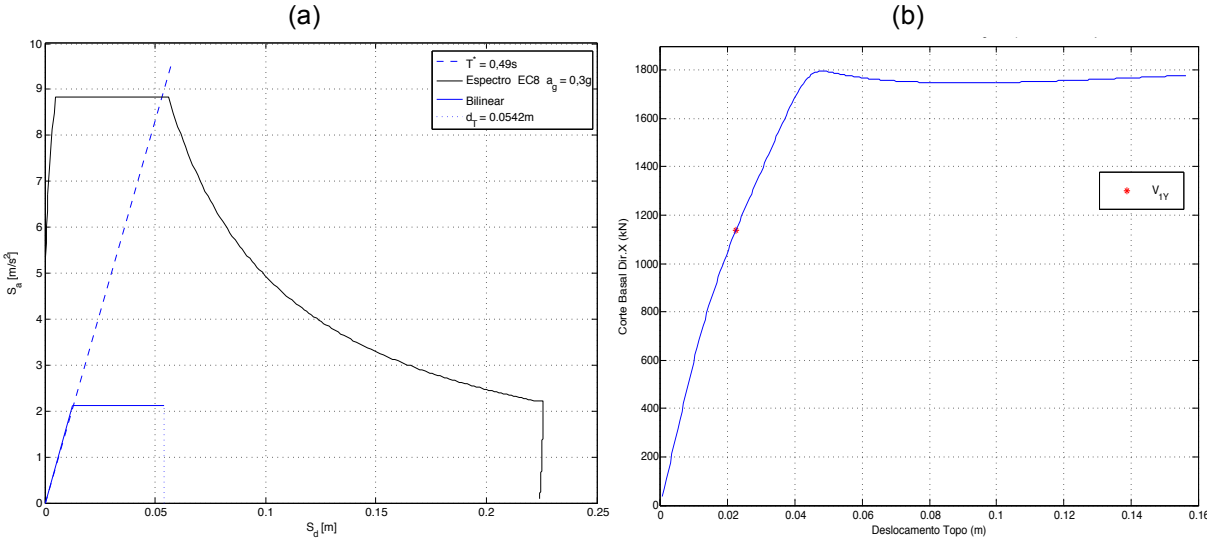

Fig. 16: IRREG structure X direction, (a) Target displacement in SDOF system and (b) Capacity Curve until target displacement in MDOF system.

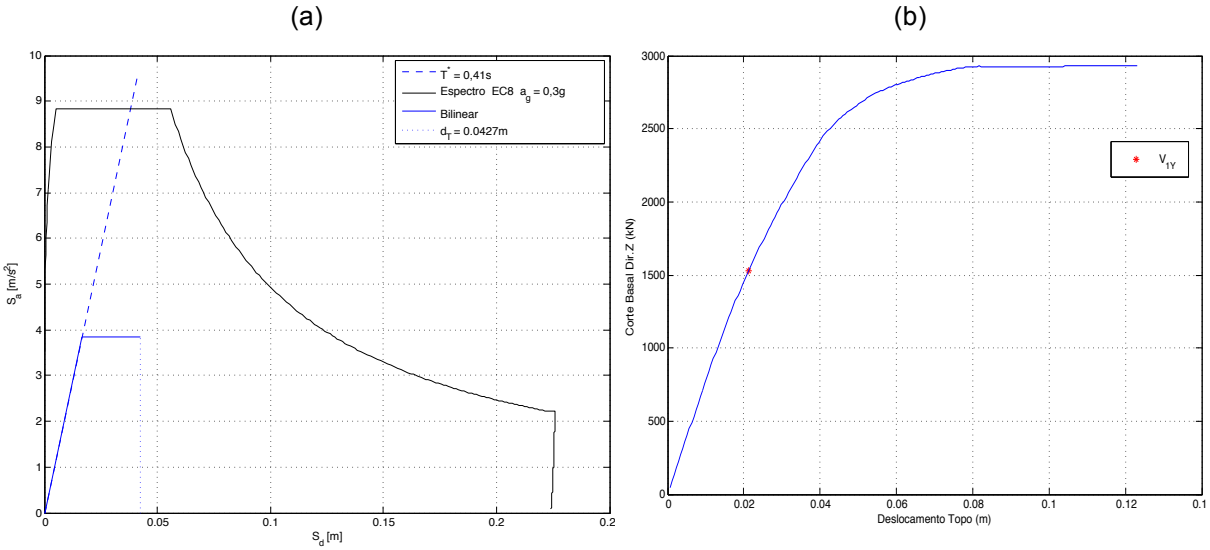

Fig. 17: IRREG structure Z direction, (a) Target displacement in SDOF system and (b) Capacity Curve until target displacement in MDOF system.

Table 8 compares the target top displacement for the N2 method performed on both directions with the reference value displayed in the last column. Given that the N2 method is an iterative process, the reference value is considered as the first iteration of such process implemented on both directions. **Fig. 18** and **19** display the results of seismic assessment in terms of (a) horizontal displacements and (b) inter-storey drifts along height for X direction and Z direction, respectively. Also for the irregular structure these figures reveal that the maximum inter-storey drifts occur in the first storey.

The evaluation of the following table and figures indicate that the seismic demand is below the structures capacity in both directions and that in Z direction, Frame 1 has the maximum values.

Table 8: IRREG structure, horizontal top displacements

		δ_{target} (m)			Limit δ_{top} (m) [0.025*H]
IRREG	Dir. X	0.156			0.288
	Dir. Z	0.122 [CM]	Frame 1	0.157	
			Frame 3	0.103	
			Frame 2	0.089	

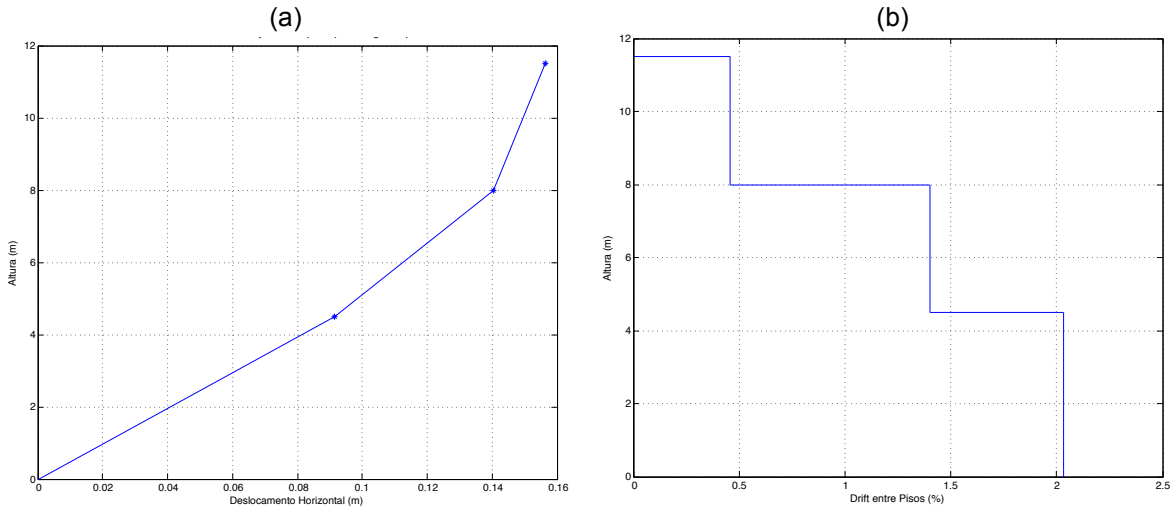

Fig. 18: IRREG structure X direction graphs for Target displacement, Frame 4, (a) Maximum horizontal displacements and (b) Inter storey drifts.

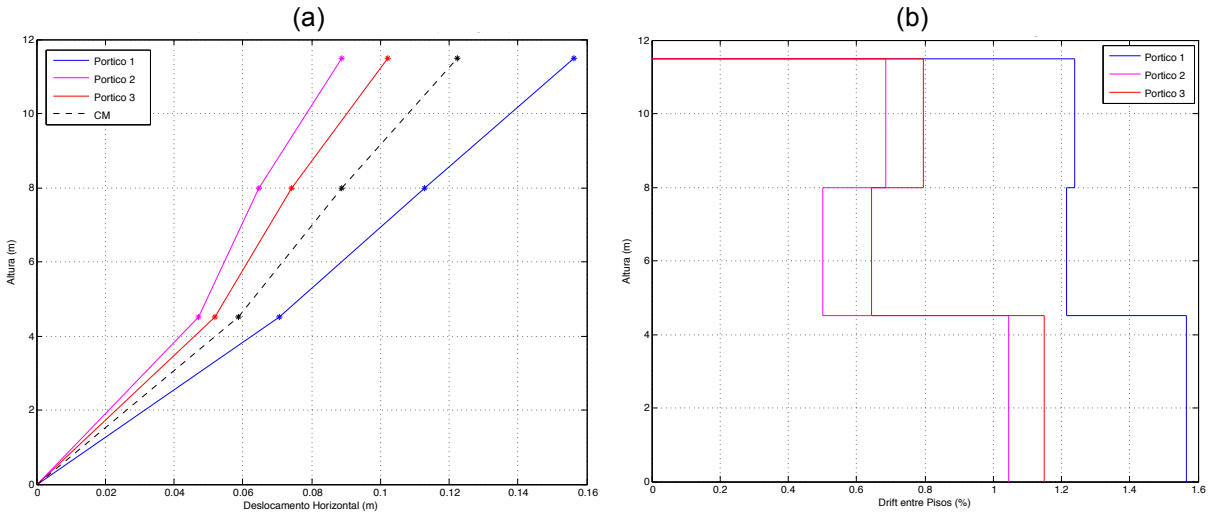

Fig. 19: IRREG structure Z direction graphs for Target displacement, (a) Maximum horizontal displacements and (b) Inter storey drifts.

Fig. 20a and **20b** illustrate the diagonals' axial force *vs.* top displacement (braces in tension and compression) for each storey and it is also depicted the corresponding target displacement for X direction and Z direction, respectively. For Z direction is illustrated the graph of Frame 1. It is worth noticing for this direction that all diagonals are performing in the inelastic range, which indicates ductile frames of the IRREG structure.

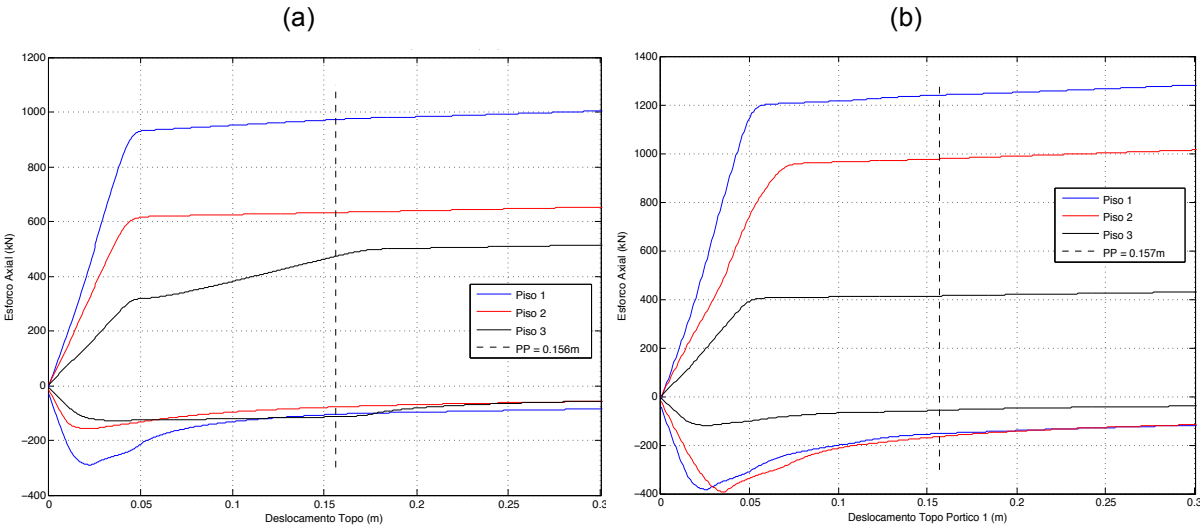

Fig. 20: IRREG structure, Diagonals response (axial force *vs.* top displacement) and representation of the corresponding target displacement in (a) X direction and (b) Z direction (Frame 1)

3.4 Time-history analysis

The selected fifteen records were scaled to match the EC8 Type 1 response spectrum used in the seismic design of both structures as illustrated in **Fig. 21a**. The *Coalinga* record illustrated in **Fig. 21b** was the only record that successfully reached its completion.

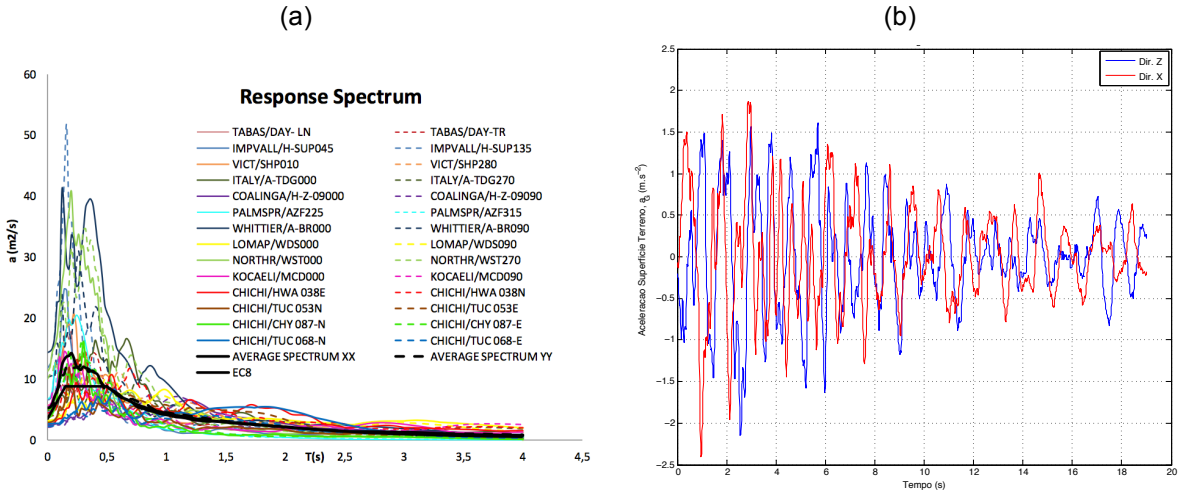

Fig. 21: (a) Acceleration response spectrum of the 15 records matching EC8 Type 1 response spectrum and (b) *Coalinga* record combination on both directions.

In **Fig. 22** and **Fig. 23** the ratio between the axial force in the diagonal (N_{ED}) and the design resistance of the diagonal, i.e. tensile yield resistance ($N_{pl,Rd}$) *vs.* the ratio between the axial deformation in the diagonal (Δ) and tensile yield axial deformation of the diagonal (Δ_y) is shown for Z direction and X direction for REG structure.

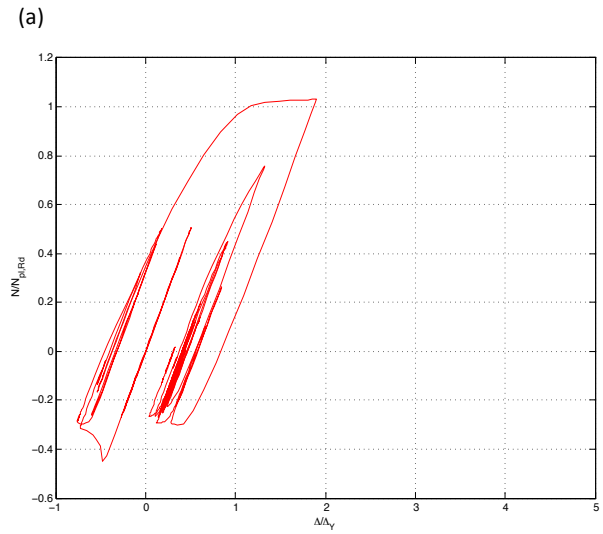

Fig. 22: REG structure, Z direction, Hysteretic pinned-end brace response: (a) Storey 3, (b) Storey 2 and (c) Storey 1.

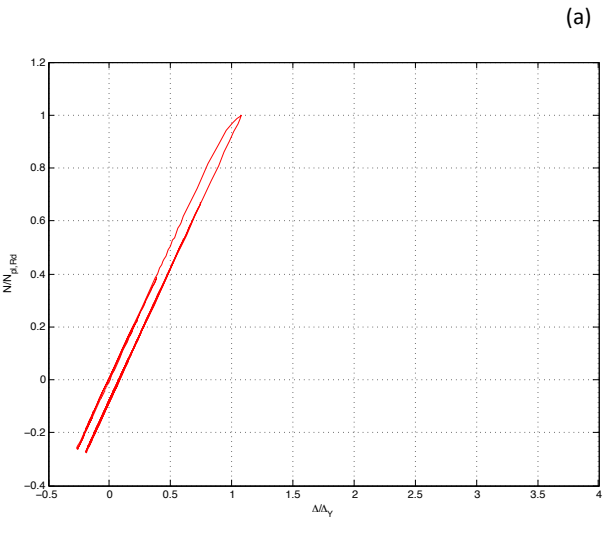

Fig. 23: REG structure, X direction, Hysteretic pinned-end brace response: (a) Storey 3, (b) Storey 2 and (c) Storey 1.

The energy dissipation capability of the diagonal under cyclic loading corresponds to the area enclosed by the hysteresis loops shown above. The storey 1 is clearly subjected to the highest energy dissipation from all diagonals of the respective frame. It is worth noticing the asymmetry in the hysteretic response of the pinned-end braces, given by the buckling in compression and yielding in tension.

4. Conclusion

The work herein presented was addressed to the seismic design and seismic performance evaluation of a regular and irregular in plan three storey CBF structures both laterally restrained.

The seismic design is carried out following the IFBD procedure in accordance with EC8´s design criteria and detailing rules. The use of the IFBD procedure lead to more realistic and lower values of behaviour factor on both structures than the value of 4 suggested by EC8, which indicates limited level of inelastic demand to be imposed on both structures in comparison to the level proposed by EC8.

The seismic performance evaluation developed has proven to be crucial on making an intervention in the seismic design of the REG structure, clearly showing the advantages related with the use of non-linear analysis in addition to the force-based procedure used in the design. In the X direction of this structure the inter-storey drift of storey 1 surpasses the 2.5% limit prescribed, which leads to the following proposal: the brace's gusset plate connection to become focus of thorough detailing in seismic design in order to reduce the clear length of braces measured between the gusset plates leading to lower slenderness ratio. REG structure's frames in Z direction and the frames in both directions of IRREG structure exhibit seismic demand below the frame's capacity. Both set of structures are ductile due to good energy dissipation capability of its diagonals.

The developed OpenSees code for both structures was precursor at seismic evaluation in a tridimensional environment for CBF structures.

References

Brandonisio, G. et al., 2012. Seismic design of concentric braced frames. *Journal of Constructional Steel Research*, 78, pp.22–37.

CEN, 2002. EN1990. Eurocode 0: Basis of structural design.

CEN, 2005. EN 1993-1-1, Eurocode 3: Design of steel structures - Part 1: general rules, seismic actions and rules for buildings.

CEN, 2004. EN1998-1-3, Eurocode 8 : Design of structures for earthquake resistance - Part 1 : General rules, seismic actions and rules for buildings.

Inc., C. and S., 2014. SAP2000 v17

Cruz, N. – “Dimensionamento e Avaliação sísmica de um edifício metálico irregular contraventado de 3 pisos”, Dissertação para obtenção do Grau de Mestre em Engenharia Civil, Instituto Superior Técnico, Portugal, 2015

Krawinkler, H. & Seneviratna, G.D.P.K., 1998. Pros and cons of a pushover analysis of seismic performance evaluation. *Engineering Structures*, 20(4-6), pp.452–464.

Nogueiro, P., Bento, R. & Silva, L.S. da, 2006. Evaluation of the ductility demand in partial strength steel structures in seismic areas using non-linear static analysis. In *Proceedings of the XI International Conference Metal Structures*.

Pacific Earthquake Engineering Research Center, 2006. OpenSees: Open System for Earthquake Engineering Simulation. University of California, Berkeley.

Tremblay, R., 2000. Seismic design and behaviour of concentrically braced steel frames. In *2000 North American Steel Construction Conference - AISC*.

Uriz, P., Filippou, F.C. & Mahin, S. a., 2008. Model for cyclic inelastic buckling of steel braces. *Journal of Structural Engineering*, 134(4), pp.619–628.

Villani, A., Castro, J.M. & Elghazouli, A.Y., 2009. Improved seismic design procedure for steel moment frames. *STESSA 2009: Behaviour of Steel Structures in Seismic Areas,* 2009, 673-678.